

09,16

## Second phosphorescence of synthetic HPHT diamonds

© A.V. Spirina<sup>1</sup>, V.I. Solomonov<sup>1</sup>, M.P. Popov<sup>2</sup>, M.A. Ivanov<sup>1</sup>, V.V. Kuptsova<sup>1</sup>

<sup>1</sup>Federal State Budgetary Institution of Science  
Institute of Electrophysics, Ural Branch of the Russian Academy of Sciences,  
Ekaterinburg, Russia

<sup>2</sup>Federal State Budgetary Educational Institution of Higher Education „Ural State Mining University“,  
Ekaterinburg, Russia

E-mail: rasuleva@iep.uran.ru

Received November 20, 2025

Revised November 22, 2025

Accepted December 2, 2025

The pulsed cathodoluminescence of synthetic HPHT diamonds excited by an electron pulse beam was studied at room temperature in air. The luminescence spectra of all diamonds contain a single non-elementary band; its maximum varies in the range from 490 to 504 nm. After turning off the electron beam, a second phosphorescence centered at 489 nm is observed. The kinetics of luminescence decay on the long-wavelength wing of the band at 520 nm was studied. Five characteristic times were obtained, three of which,  $\tau_1 = 0.18$ ,  $\tau_2 = 2$  and  $\tau_3 = 18$  ms, are related to the kinetics of the A-band, while the other two,  $\tau_4 = 190$  ms and  $\tau_5 = 4.5$  s, are related to the emission of C<sub>2</sub> molecule. It is formed from interstitial carbon atoms under the action of high pressure and temperature during the synthesis of diamonds by the HPHT method and their embedding into cavities with tetrahedral and hexagonal symmetry.

**Keywords:** pulsed cathodoluminescence, synthetic diamond, HPHT diamond, spectrum, interstitial carbon atom, kinetics, long-time emission.

DOI: 10.61011/PSS.2025.12.63087.326-25

### 1. Introduction

The luminescence of diamonds has been well studied, and the nature of most of its luminescence centers has been determined [1–3]. In particular, in the X-ray and cathodoluminescence (XRL and CL) spectra of natural and synthetic diamonds, a wide structureless A-band with a maximum varying in the range of 400–480 nm is often observed [3–6]. The method of XRL diamond separation is based on the excitation of this particular band [7]. The illumination of the A-band has complex kinetics — it exhibits slow ( $> 10$  ms) and fast ( $< 1$  ms) components [6,8,9]. It is shown in Ref. [9] that in diamonds synthesized by the high pressure high temperature (HPHT) method, a phosphorescence band, which is part of the A-band, is observed during photoexcitation with a wavelength of 235 nm, as well as in CL, and the position of its maximum depends on the crystal plane, from which the spectrum is recorded. At room temperature of the samples, the maximum phosphorescence band from the crystal plane B {001} falls at a wavelength of 484 nm, and from the plane C {111} — at 494 nm, and the phosphorescence band with a maximum fades at a lower energy faster than the maximum at a higher energy.

When excited by ultraviolet radiation, luminescence is observed in a wider spectral range [10–12]. In the blue region of photoluminescence (PL), the glow of the N3 center with 415.2 nm phononless line and 40 ns a decay time is observed; the glow of the S and H family of

centers is observed in the yellow-green region. The S1 center gives two phononless lines at 503.4 and 510.7 nm with decay times of 3.2 and 10.4 ms, respectively. The S2 center emits three phononless lines, two of which, 477.8 and 489.1 nm, have the same characteristic time 3.5  $\mu$ s, and the third line at 523.3 nm has a characteristic time of 0.24 ms. The centers H3 and H4 with phononless lines at 496.7 and 503.2 nm have times 17–19 ns. Also, in the PL spectra of a number of diamond samples, along with these lines, a wide band of phosphorescence is recorded with a maximum in the green region of the spectrum at 523 nm [9,10]. This band, which is well distinguished when the spectrum detection is delayed by 20  $\mu$ s relative to the excitation cutoff, is associated in Ref. [10] with the presence of S2- and S3-defects in samples of natural diamonds from deep horizons of the „Mir“ and „Internationalnaya“ pipes. The same band was dominant in the PL, XRL, and CL spectra of microcrystalline diamond synthesized by the HPHT method [11]. The authors associate it with H3 defects, and the spectral characteristics of this phosphorescence band differ from those of the phosphorescence in the A-band.

In the pulsed CL (PCL) of synthetic diamonds produced by the HPHT method, a wide structureless luminescence band is observed with a maximum shifting from 490 to 504 nm from sample to sample and having complex kinetics at room temperature with several time components, one of which is units of seconds. The purpose of this paper is to study the nature of this luminescence.

## 2. Equipment and research objects

102 samples of round (KR-57) colorless synthetic faceted and polished diamonds of different quality weighing 0.028–0.380 ct, produced by the HPHT method, were studied. The PCL of the samples was excited and examined using the KLAVI [13]. The samples were irradiated in air at room temperature with an electron beam of 2 ns duration with a current density of 130 A/cm<sup>2</sup> at an average electron energy of 170 keV. The PCL spectrum was recorded in the range of 350–850 nm in the time integration mode:

$$I(\lambda) = \frac{1}{N} \int_{T_1}^{T_2} i(\lambda, t) dt,$$

where  $i(\lambda, t)$  is current luminescence intensity,  $T_1$  and  $T_2$  is the start and end of recording,  $\Delta T = 50$  ms is the exposure,  $N = 40$  is the number of pulses for which spectral information was averaged. Luminescence was recorded in air at room temperature from the entire irradiated surface of the sample. The wavelength measurement error did not exceed 0.5 nm.

To study the kinetics of luminescence bands, the radiation flux from the sample was output via a multicore fiber to the input of a spectrometric system produced by „OKB SPEKTR“ LLC (St. Petersburg) based on the monochromator MDR-41 and the FEU-100 photomultiplier, the signal from which was supplied to the input impedance of the Keysight DSOX2014A digital oscilloscope via a 1.5 m coaxial cable with a wave resistance of 50  $\Omega$ . The kinetic hardware function of the measuring circuit had the form of a decreasing exponent with a characteristic time  $\tau = RC = 169 \mu\text{s}$ , where  $R = 1 \text{ M}\Omega$  is the input impedance of the oscilloscope,  $C$  is the electrical capacity. In such a circuit, the measured voltage drop  $U_R$  at resistance 1 M $\Omega$  is a convolution of the photocurrent caused by luminescence and the kinetic hardware function. The method of calculating kinetic parameters in this case includes the procedure of deconvolution of the convolution of two signals [14]. The wavelength positioning error in kinetic measurements was no worse than  $\pm 0.3$  nm with a spectral hardware function width of 4 nm.

Photoluminescence spectra were obtained using a Horiba LabRam HR800 Evolution RAMAN spectrometer when excited by laser radiation with a wavelength of 488 nm (Ar laser) in the wavelength range of 487–900 nm when samples were cooled to 83 K. The spectra were recorded using a Czerny-Turner monochromator with an 1800 gr/mm diffraction grating and a multichannel silicon electrically cooled CCD detector.

Infrared absorption spectra (IR spectra) in the region of 600–4000 cm<sup>-1</sup> were recorded in the „reflection“ mode using a MultuScope infrared microscope combined with a Spectrum One spectrometer (Perkin Elmer). Averaging was performed using 200 interferograms with a spectral resolution of 4 cm<sup>-1</sup>.

## 3. Results and their discussion

Figure 1, *a* shows typical PCL spectra of samples of synthetic HPHT diamonds recorded during action of an electron beam. Luminescence consists of wide bands, the contours of which in the scale of wave numbers (cm<sup>-1</sup>) are described by the Gauss curve. For demonstration, the spectra corresponding to the minimum (490.0 nm, curve 1) and maximum (504.0 nm, curve 2) wavelengths of luminescence bands among all recorded spectra were selected. The chaotic distribution of spectral parameters, such as the position of the band and its width, for all the studied samples is shown in Figure 1, *b*, where the numbers indicate the points corresponding to the spectra shown in Figure 1, *a*.

After the excitation cutoff, intense blue phosphorescence was observed in all diamonds for several seconds. To separate the structure and find the parameters of the phosphorescent band, the spectra of ten randomly taken samples were recorded with a delay of 1, 3, 5, and 7 s

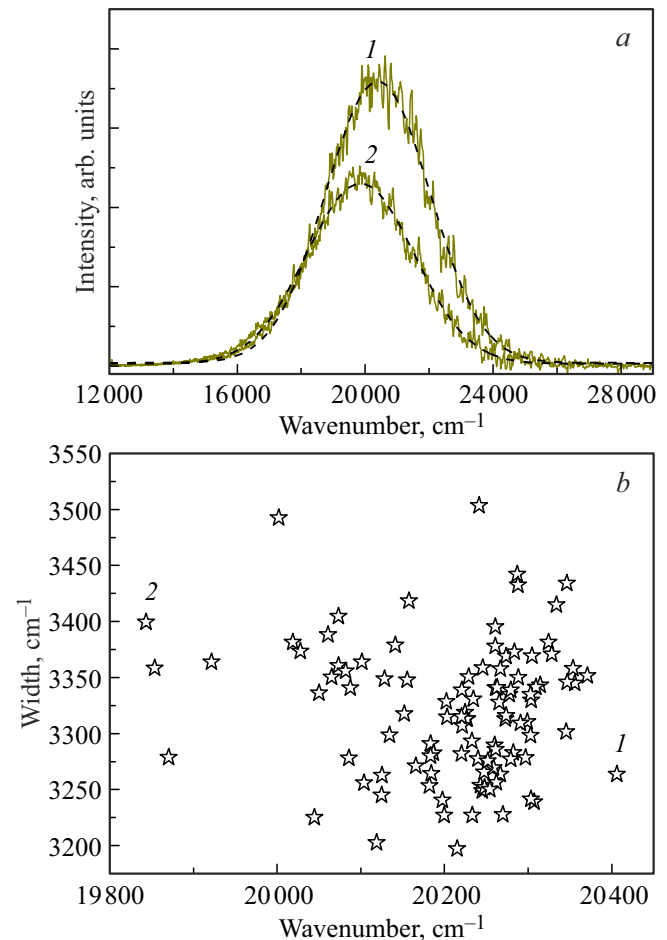


**Figure 1.** *a*) Characteristic PCL spectra of synthetic diamonds corresponding to the lowest (curve 1) and maximum (2) wavelengths of luminescence band maxima recorded among 102 samples; *b*) distribution of the parameters of the bands (position and width) obtained by approximating the Gauss curve.

Statistical weights of exponential functions with corresponding characteristic times on different time scales

| Time scale per division, ms | $\tau_1 = 0.18$ ms | $\tau_2 = 2.0$ ms | $\tau_3 = 18$ ms | $\tau_4 = 190$ ms | $\tau_5 = 4.5$ s |
|-----------------------------|--------------------|-------------------|------------------|-------------------|------------------|
| 10                          | 0.81               | 0.13              | 0.06             | –                 | –                |
| 100                         | –                  | 0.72              | 0.20             | 0.08              | –                |
| 500                         | –                  | –                 | 0.75             | 0.17              | 0.08             |

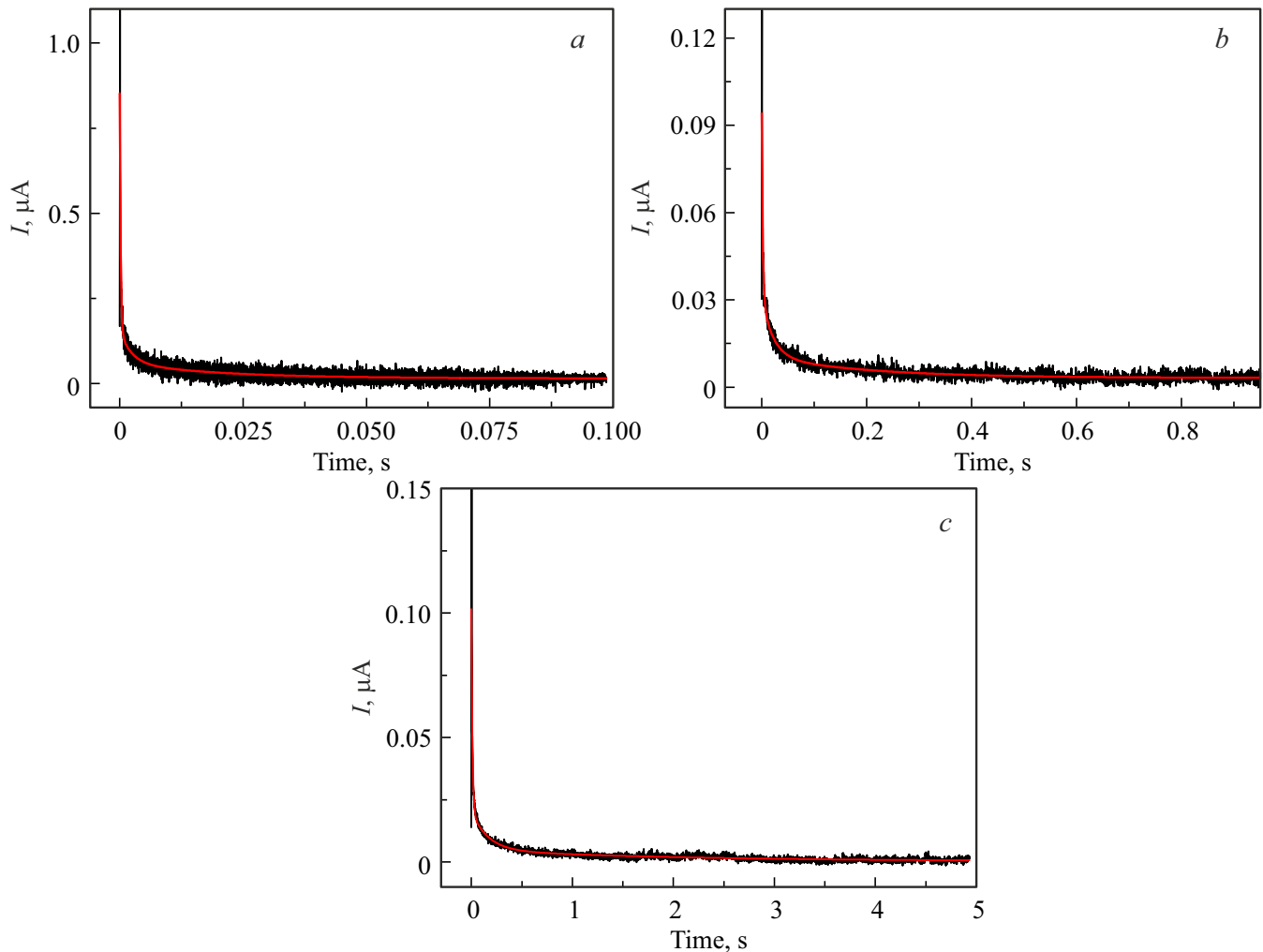


**Figure 2.** Kinetic dependences recorded on the oscilloscope time scales *a*) 10, *b*) 100 and *c*) 500 ms, and their approximations (red curves).

after the electron beam was cut off. The position, width, and intensity of the spectral bands were determined by approximating the Gauss curve. The wavelengths of the second phosphorescence bands in all samples shifted to the short-wavelength region by an amount from 5 to 10 nm, and the bands themselves broadened by 2–5 nm relative to the luminescence band of the same samples, but recorded during the action of the electron beam. In this case, the wavelength of the phosphorescence band with an accuracy of 1 nm was 489 nm. The phosphorescence decay time was

also estimated by drawing an envelope in the form of a decaying exponential function based on the band intensities measured at 1, 3, 5, and 7 s after the excitation cutoff the excitation. The typical time ranged from 2 to 5.5 s.

To further study this luminescence center, kinetic curves were recorded not at the band maximum but at its long-wavelength wing (520 nm), where the kinetics the A-band and also the overlapping centers with it are more likely to be detected. The waveforms were recorded at time scales of 10, 100, and 500 ms per division. Their deconvolution

is shown in Figure 2 for all time scales. All kinetic curves have the same type.

Processing of these signals has shown that they are approximated by the sum of three exponential functions for each time scale:

$$I = I_1 \exp\left(-\frac{t}{\tau_1}\right) + I_2 \exp\left(-\frac{t}{\tau_2}\right) + I_3 \exp\left(-\frac{t}{\tau_3}\right)$$

for a time scale of 10 ms per division,

$$I = I_4 \exp\left(-\frac{t}{\tau_2}\right) + I_5 \exp\left(-\frac{t}{\tau_3}\right) + I_6 \exp\left(-\frac{t}{\tau_4}\right)$$

for a time scale of 100 ms per division,

$$I = I_7 \exp\left(-\frac{t}{\tau_3}\right) + I_8 \exp\left(-\frac{t}{\tau_4}\right) + I_9 \exp\left(-\frac{t}{\tau_5}\right)$$

for a time scale of 500 ms per division.

In total, diamonds have 5 characteristic times, the average values of which are given in the table; the corresponding time scale and the statistical weight introduced into the integral intensity of the band by each exponential function are indicated here.

It can be seen that a higher statistical weight corresponds to a shorter defined for each time scale.

The recording of kinetics in different time ranges and the further use of the time curve processing technique [14] made it possible to record three components of the A-band:  $\tau_1$  (0.18 ms),  $\tau_2$  (2.0 ms) and  $\tau_3$  (18 ms), each of which has a high statistical weight when time scales an oscilloscope of 10 ms, 100 ms and 500 ms.

Not all samples allowed the characteristic time  $\tau_4$  to be recorded, and the statistical weight of the exponential function that includes the parameter  $\tau_5$  is negligible. In this case, the parameter  $\tau_5$  has the same value that was obtained when recording the spectrum at 1, 3, 5, and 7 s after the excitation cutoff along the curves enclosing the maxima of the phosphorescence bands.

The recording of photoluminescence spectra when excited by an Ar laser with a wavelength of 488 nm showed similar spectra (Figure 3). The recorded range captures two orders of Raman scattering, which is indicated in the figure as shaded areas. Weak lines at 537, 575, 585, and 637 nm are observed in the spectra associated with nitrogen vacancy defects ( $N_3V^-$ ), ( $NV^0$ ), ( $N_3V^0$ ), and ( $NV^-$ ) respectively [1]. Some samples exhibit a doublet in the near-infrared region at 883–884 nm (Figure 3, curve 2) corresponding to the nickel center  $NiV^+$  [1], formed under conditions of HPHT synthesis. There were no other features.

In the IR absorption spectra, on the contrary, various lines were present from sample to sample (Figure 4). In addition to lattice absorption, the spectra show lines characteristic of A-, B1- and C-defects, which are associated with the presence of nitrogen impurity in the samples [1]; lines showing the presence of boron impurity in the samples (B); as well as a structured system of Y-defects, which is

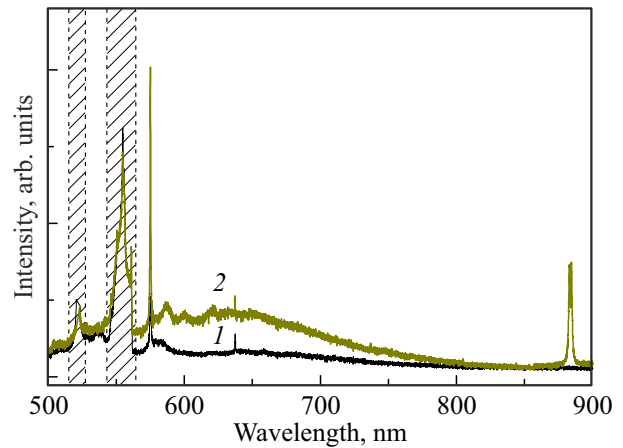


Figure 3. Photoluminescence spectra of HPHT diamonds.

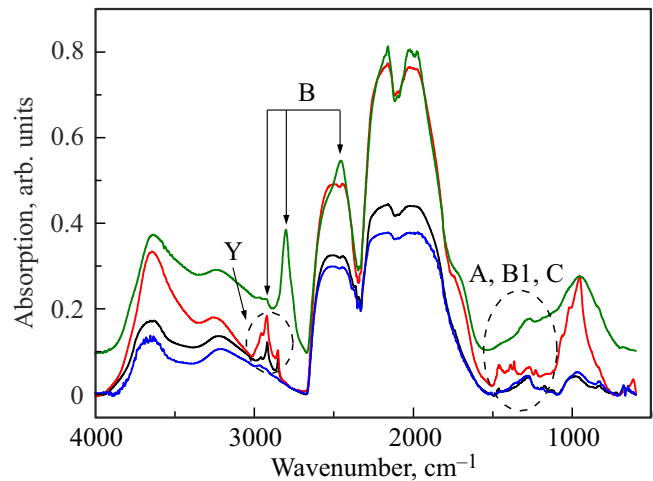
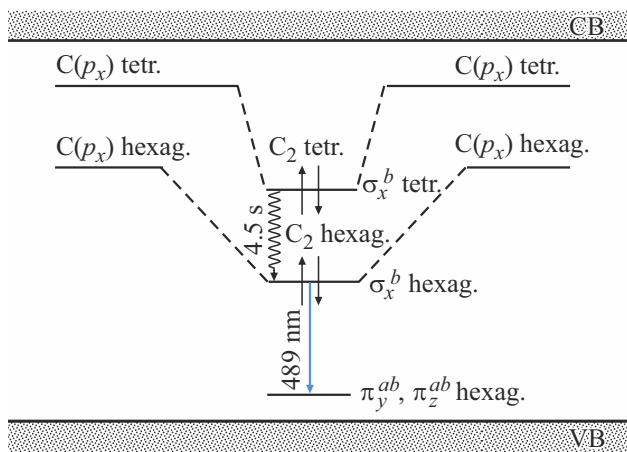


Figure 4. Infrared absorption spectra of synthetic HPHT diamonds.

observed in diamonds having zones saturated with various inclusions [1,15].

Thus, phosphorescence is not related to the impurity composition, and its stability in different diamond samples (position at 489 nm) indicates that this center is formed due to the formation of the same intrinsic defect in the crystal lattice for all phosphorescent samples.

There are two highly symmetric interstitial positions in the diamond lattice: tetrahedral and hexagonal. Calculations of the electronic, vibrational, and structural characteristics of interstitial carbon atoms were performed using numerical modeling methods [15], which showed that the total energy of a diamond with a neutral carbon atom in a hexagonal position is significantly less than in a tetrahedral position [15,16]. It is stated in Refs. [15,17] that most of the data on interstitial carbon atoms for models of the microstructure of the centers were obtained using electron paramagnetic resonance (active centers R1, R2, O3). The manifestation of an interstitial carbon atom in the infrared



**Figure 5.** Scheme of formation of the emitting center associated with the second phosphorescence.

spectra of natural diamonds (lines at 1530, 1570  $\text{cm}^{-1}$ ) not observed in our spectra, is considered in Ref. [18]. Absorption at 1.685 and 1.859 eV is also associated with the interstitial defect [15]. But it is still believed that these defects are poorly understood. There are no direct, unambiguously interpreted experimental results concerning the properties of intrinsic interstitial atoms. This is primarily due to the fact that the interstitial carbon atom has high mobility in diamond even at room temperature [15,17].

In this paper, we study HPHT samples that were grown under high pressure and temperature conditions, where interstitial intrinsic defects necessarily occur. Moving through the crystal, carbon atoms interact with each other, which leads to the formation of a molecule  $\text{C}_2$  in the diamond structure. According to the theory of molecular orbitals, two atomic carbon ( $p_x$ ) orbitals with the same energy and the same tetrahedral symmetry form a molecule  $\text{C}_2$  (tetr.) with bonding  $\sigma_x^b$  and antibonding  $\sigma_x^{ab}$  molecular orbitals. The same thing happens with carbon  $p_x$ -orbitals of hexagonal symmetry, which are energetically located below. A defect  $\text{C}_2$  (hexag.) is formed with its  $\sigma_x^b$ - and  $\sigma_x^{ab}$ -orbitals (Figure 5). The allowed transition in the orbital quantum number from the bonding orbital  $\sigma_x^b$  to the states with antibonding orbitals  $\pi_y^{ab}$  or  $\pi_z^{ab}$  occurs with luminescence emission with a wavelength of 489 nm.

However, this process is extended in time by an average of 4.5 s — this is the time of nonradiative energy transfer from  $\sigma_x^b$  (tetr.) to  $\sigma_x^b$  (hexag.), since the formed molecules  $\text{C}_2$  are positionally separated from each other. After emission, the  $\text{C}_2$  molecule dissociates to form mobile carbon atoms.

The time  $\tau_4$  (190 ms), as mentioned above, was not recorded for all samples. We assume that the wide band of pulsed cathodoluminescence is formed by radiation lines, including those of  $\text{C}_2$  corresponding to the Swan system [18]. In this system, for a free molecule, the wavelength of the most intense vibrational transition (0 – 0)

is 516.5 nm. Kinetic measurements were performed at a wavelength of 520 nm. Given the dispersion of the device and the fact that the  $\text{C}_2$  molecule in the crystal is mobile and a shift in the line position is possible, it is likely that in some cases this radiation falls into the measured range, and in some cases it is not observed. According to Ref. [18] the electronic transfer is forbidden according to the selection rules, which, in turn, determines the long lifetime of the top level.

## 4. Conclusion

The PCL spectrum of diamonds synthesized by the HPHT method exhibits a band that changes its position in the range of 490–504 nm. After the excitation cutoff, a second phosphorescence is recorded in all 102 studied samples, the wavelength of which is 489 nm. The kinetics of the entire band is complex. Five characteristic times were recorded on different time scales of the oscilloscope, three of them correspond to the kinetics of the A-band (0.18, 2 and 18 ms). The other two times are associated with the formation of intrinsic defects, which are interstitial active carbon atoms capable of interacting with each other to form the  $\text{C}_2$  molecule. The structural separation of such defects occurs due to the presence of two highly symmetrical interstitial positions, tetrahedral and hexagonal, between which nonradiative energy transfer occurs during 4.5 s followed by radiation at 489 nm. In addition, the PCL band is formed by emission lines of molecular carbon from the Swan system with a characteristic lifetime of the electron level 190 ms.

## Conflict of interest

The authors report no conflict of interest.

## References

- [1] Diamond: Genesis, Mineralogy and Geochemistry, v. 88 / Eds K. Smit, S. Shirey, G. Pearson, T. Stachel, F. Nestola, T. Moses. Walter de Gruyter GmbH & Co KG (2025).
- [2] B. Dischler. Handbook of Spectral Lines in Diamond, v. 1: Tables and Interpretations. Springer Science & Business Media, London–New York (2012).
- [3] G.N. Bezrukov, G.B. Boki, Yu.A. Klyuev, A.M. Naletov, V.I. Nepsha. Prirodnye i sinteticheskie almazy. Nauka, M. (1986) (in Russian).
- [4] S.G. Mikhailov, V.I. Solomonov. Optika i spektroskopiya **80**, 5, 781 (1996) (in Russian).
- [5] E.I. Lipatov, V.M. Lisitsyn, V.I. Oleshko, V.F. Tarasenko. Russ. Phys. J. **50**, 1, 52 (2007). <https://doi.org/10.1007/s11182-007-0005-8>
- [6] V.P. Mironov. V sb: Trudy IX mezhdunarodnoj shkoly-seminara po lyuminescencii i lazernoj fizike / Pod red. S.N. Bagaeva, N.A. Borisevicha, E.F. Martynovicha. Irkutsk State University, Irkutsk (2005). p. 102 (in Russian).

- [7] A.I. Bakhtin, B.S. Gorobets. Opticheskaya spektroskopiya mineralov i rud i ee primeneniye v geologorazvedochnykh rabotakh. Izd. Kazanskogo universiteta, Kazan (1992) (in Russian).
- [8] E.F. Martynovich, L.V. Ice cream maker, I.A. Parfianovich. FTT **15**, 4, 927 (1973) (in Russian).
- [9] J. Zhao, B.L. Green, M.E. Newton, B.G. Breeze. Phys. Rev. B **108**, 16, 165203 (2023).
- [10] V.A. Chanturia, I.J. Bunin, G.P. Dvoichenkova, O.E. Kovalchuk. Fiziko-tehnicheskie problemy razrabotki poleznykh iskopaemykh, 2, 109 (2016) (in Russian).
- [11] O.G. Lysenko, V.I. Grushko, E.I. Mitskevich, G.D. Ilnitskaya, A.Yu. Boyarintsev, Yu.D. Onufriev, V.F. Popov, L.G. Levchuk, N.M. Kozyuchits, M.S. Rusetsky, V.V. Lysakovsky, S.A. Ivakhnenko. Nadtverdi materiali 1, 23 (2019) (in Russian).
- [12] F.A. Stepanov, A.S. Emelyanova, A.L. Rakevich, V.P. Mironov, D.A. Zedgenizov, V.S. Shatskiy, E.F. Martynovich. Bull. RAS: Phys. **81**, 9, 1099 (2017).
- [13] V.I. Solomonov, S.G. Michailov, A.I. Lipchak, V.V. Osipov, V.G. Shpak, S.A. Shunailov, M.I. Yalandin, M.R. Ulmaskulov. Laser Phys. **16**, 1, 126 (2006).  
<https://doi.org/10.1134/S1054660X06010117>
- [14] V.I. Solomonov, A.V. Spirina, A.S. Makarova, A.I. Lipchak, A.V. Spirin, V.V. Lisenkov. J. Optic. Technol. **89**, 12, 728 (2022).
- [15] E.A. Vasiliev. Defektoobrazovanie v almaze na raznykh etapakh kristallogeneza. Avtoref. dokt. diss. Sankt-Peterburgskiy gornyy universitet, SPb (2021) (in Russian).
- [16] V.K. Bazhenov, I.M. Vikulin, A.G. Gontar. Sov. Phys. Semicond.-USSR **19**, 8, 829 (1985).
- [17] V.S. Vavilov, A.A. Gippius, E.A. Konorova. Elektronnyye i opticheskie processy v almaze. Nauka, M. (1985) (in Russian).
- [18] R.W.B. Pearse, A.G. Gaydon. The Identification of Molecular Spectra. Chapman & Hall Ltd., London (1941).

*Translated by A.Akhtyamov*